Structure of Microporous Polypropylene Sheets Containing $CaCO_3$ Filler

SATOSHI NAGŌ,* SHUNICHI NAKAMURA, and YUKIO MIZUTANI

Tokuyama Soda Co., Ltd., Tokuyama-City 745, Japan

SYNOPSIS

The microporous polypropylene sheets were prepared by biaxially stretching polypropylene sheets containing $CaCO_3$ filler (particle size, 0.08–3.0 μm), when the $CaCO_3$ filler content was 59% by weight and the stretching ratio was 2.8 × 1.8. The microstructure of the sheets were investigated in relation to the $CaCO_3$ particle size by a N_2 gas permeation method. (1) Effective porosity increases with decreasing mean particle size of filler. (2) The tortuosity factor of the pore is in the range of 25–40 and becomes relatively smaller with decreasing mean particle size of filler. (3) The equivalent pore size becomes relatively smaller with decreasing mean particle size of filler.

INTRODUCTION

Many investigators have so far been studying microporous film, sheet, or membrane, which were prepared by various methods as follows:

1. Sintering fine polymeric powder.[1]
2. Extracting a finely dispersed inorganic filler and organic plastisizer from substrate polymer.[2]
3. Microphase separation.[3]
4. Stretching crystalline polymer.[4–6]

Generally, the structure of microporous film, sheet, or membrane is owing to preparative procedure and also significantly affects their properties. Some investigators have studied the relation between structure and properties of the microporous film, sheet, or membrane.[7–10]

We have succeeded in the preparation of microporous sheets by biaxially stretching polymeric composite sheets containing fillers.[11–15]

In this study we report the relation between structure and properties of microporous polypropylene (PP) sheets prepared by biaxially stretching PP composite sheet containing $CaCO_3$ filler, regarding particle size of the $CaCO_3$ filler.

EXPERIMENTAL

Materials

PP was PN-120 (MFI, 1.2) from Tokuyama Soda Co., Ltd. $CaCO_3$ fillers were of commercial grade. The particle size distribution curves and transmission electron micrograph of fillers are shown in Figures 1 and 2, respectively. Liquid polyester plasticizer composed of adipic acid and propylene glycol (number-average molecular weight, 2300) were used as an additive, surface treating agent of $CaCO_3$ filler. Antioxidant used was 2,6-di-*t*-butyl-4-methylphenol.

The preparative procedures are shown below.

PP powder	39 parts
$CaCO_3$ filler	59 parts
Additives such as plasticizer and antioxidant	2 parts

↓ Mixed and then extruded at 230°C.

Pellet

↓ Extruded at 230°C.

Base sheet

↓ Stretched at 90°C in machine direction (MD; stretching ratio, ×2.8).

↓ Stretched at 120°C in transverse direction (TD; stretching ratio, ×1.8).

Microporous PP sheet

PP powder, $CaCO_3$ filler, and the additives were well mixed in advance and then pelletized with the aid of an extruder of tandem type (Nakatani Machine Co., Ltd.). Subsequently, the base sheet was molded

* To whom correspondence should be addressed.

Journal of Applied Polymer Science, Vol. 45, 1527–1535 (1992)
 CCC 0021-8995/92/091527-09$04.00

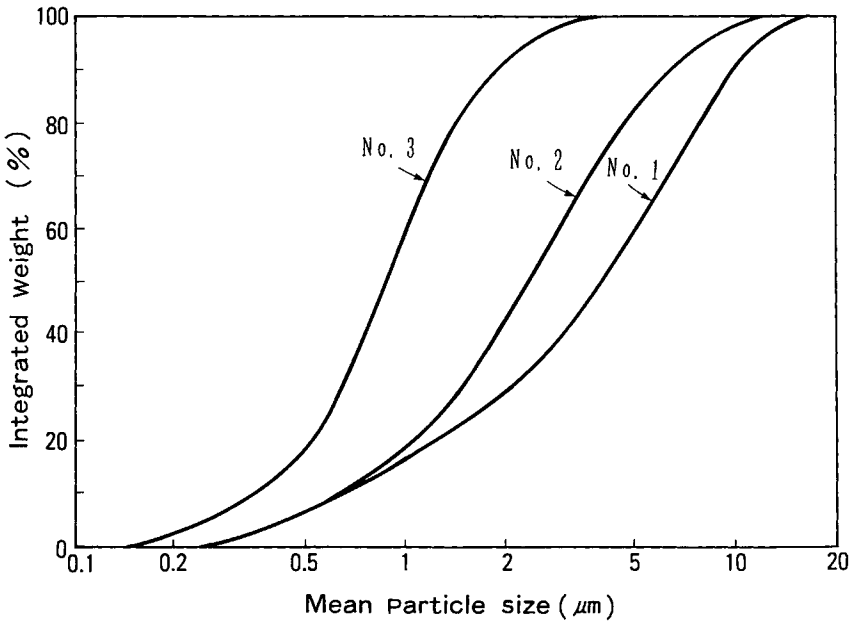

Figure 1 Particle size distributions of $CaCO_3$ fillers No. 1, No. 2, and No. 3. Mean particle size: No. 1, 3 μm; No. 2, 1.7 μm; and No. 3, 0.8 μm.

through a flat die attached on an uniaxial extruder (Iwamoto Manufacturing Co., Ltd.).

The base sheet was stretched in machine direction (MD) by using two pairs of rollers with different rotating speeds and then stretched in transverse direction (TD) by using a biaxial stretching machine of pantograph type (Type I, Brückner Co., Ltd.). The microporous PP sheets were thus prepared.

Measurements

Scanning Electron Microscopy (SEM)

The surface and cross section of the microporous PP sheets were observed with the aid of an electron microscope (Type JSM-T-220, Japan Electron Co., Ltd.).

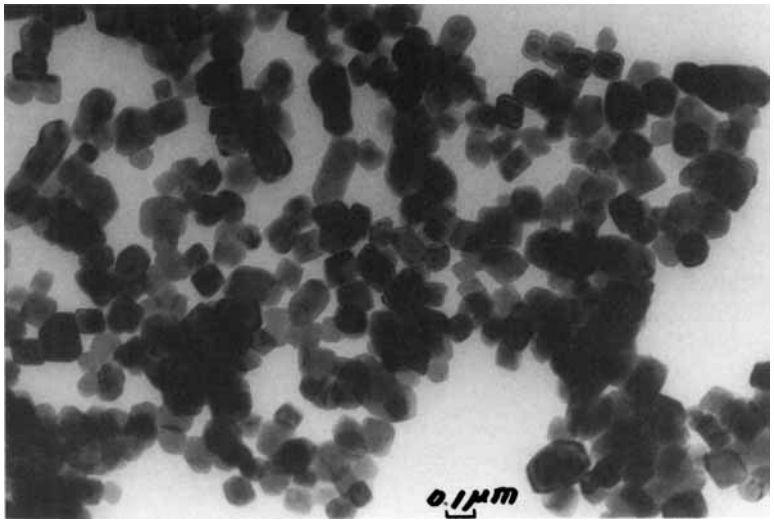

Figure 2 TEM photograph of $CaCO_3$ filler No. 4. Mean particle size, 0.08 μm.

Porosity

Apparent specific gravity (g/cm^3) was obtained by a buoyancy measurement in water and the porosity (ϵ) was calculated by using the following equation:

$$\text{Porosity } (\epsilon) = \text{void volume/volume of porous sample} = \left(\frac{d_0 - d}{d_0}\right) \times 100\ (\%) \quad (1)$$

where d_0 and d are specific gravities of the base sheet and the microporous sheet, respectively.

Pore Size Distribution

Pore size distribution was measured by using a mercury porosimeter (Type 1500, Carlo Erba Co., Ltd.).

N_2 Gas Permeability

The sample was installed between the franges sealed with rubber packing of an effective diameter of 20 mmϕ, as shown in Figure 3. N_2 gas was supplied into the chamber through pressure regulator (accuracy of 0.02 kg/cm^2). N_2 gas flux (J) was measured by a Digital Flow Meter (Model 2500 SS, Sōgō Rikagaku Industry Co., Ltd.) under definite inlet pressure (P_i) of 1.1, 1.2, and 1.3 kg/cm^2 with outlet pressure (P_0) 1 kg/cm^2. Then pressure differences of both sides of the sample (ΔP) were 0.1, 0.2, and 0.3 kg/cm^2. Mean pressure ($\bar{P}$) of both sides of the sample was calculated by the following equation:

$$\bar{P} = \frac{P_i + P_0}{2} \quad (2)$$

Maximum Pore Size

The sample impregnated with methanol was installed onto a cell as illustrated in Figure 3. A small amount of methanol was filled over the sample space and the N_2 gas pressure was increased with the rate of about 1 kg/cm^2 min. The N_2 gas pressure (P_i, kg/cm^2), when three continuous bubbles were generated from the sample, was measured. The maximum pore size (D_{max}) was calculated by the following equation (ASTM F-316):

$$D_{max}(\mu m) = 0.9388 P_i^{-1} \quad (3)$$

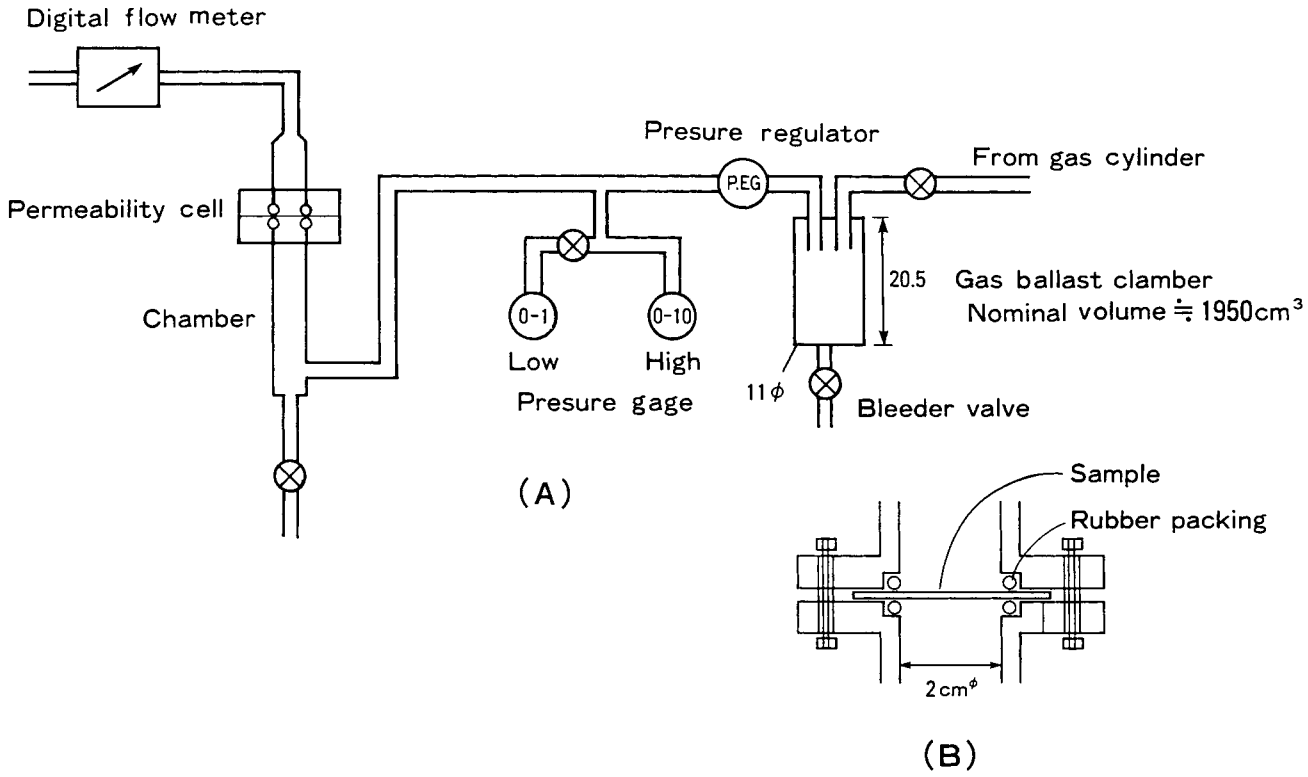

Figure 3 (a) Apparatus and (b) cell to measure gas permeability.

Table I Properties of the Microporous PP Sheets

Sample No.	$CaCO_3$ Filler: Mean Particle Size of $CaCO_3$ (μm)	$CaCO_3$ Filler: Relative Number of Particles[a]	Thickness (l) (μm)	Porosity (ϵ) (%)	Maximum Pore Size (D_{max}) (μm)
1	3.0	1	216	67	3.8
2	1.7	5.5	200	68	2.3
3	0.8	52.8	250	70	1.6
4	0.08	52,800	50	72	0.46

[a] The weight for a particle of size D_i is described by $4\pi(D_i/2)^3(d/3)$ (d is density). The number of particles, n_i, per constant weight of filler can be obtained by $4\pi(D_1/2)^3(d/3)n_1 = 4\pi(D_2/2)^3(d/3)n_2 = 4\pi(D_3/2)^3(d/3)n_3 = 4\pi(D_4/2)^3(d/3)n_4$. Therefore, the relative number of particles can be calculated by n_2/n_1, n_3/n_1, and n_4/n_1.

Determination of Pore Structure

In order to evaluate pore size of microporous polymer membrane, a gas permeability is measured in general. Yasuda et al.[7] and Cabasso et al.[9] have studied gas permeability of various millipore filters or polysulfone membrane and derived the following equations [(4)-(13)]:

$$J = K\Delta P\, l^{-1} \tag{4}$$

where J is gas flux (cm^3/cm^2 s), K is the permeability coefficient (cm^2/s), ΔP is the pressure difference across the sample, and l is the sample thickness. Permeability K is determined by the following equation:

$$K = lP_0Q(A\ \Delta P)^{-1} \tag{5}$$

where Q is the volume flow rate (cm^3/s), and A is the effective area of the sample (cm^2).

The permeability coefficient (K) of a porous membrane can be expressed as follows:

$$K = K_0 + B_0\eta^{-1}\bar{P} \tag{6}$$

where K_0 is the Knudsen permeability coefficient (cm^2/s), and η is the viscosity of the gas (s/cm^2).

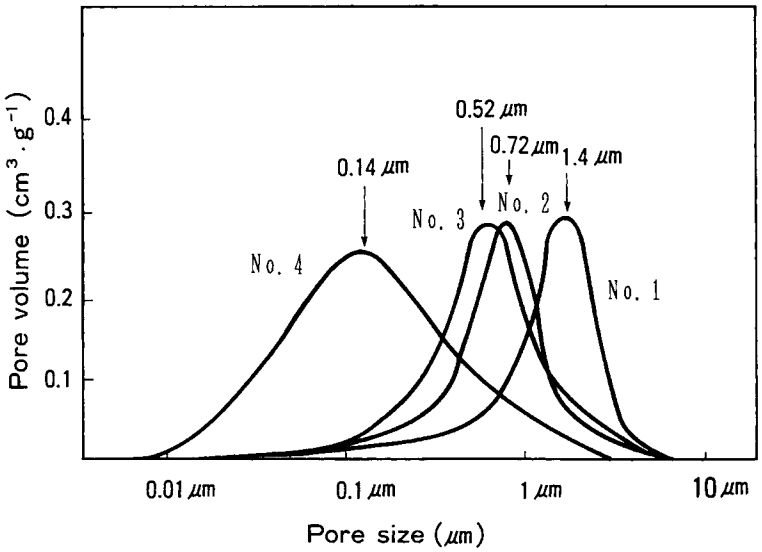

Figure 4 Pore size distribution of biaxially stretched microporous sheet. Numbers correspond to the samples shown in Table I.

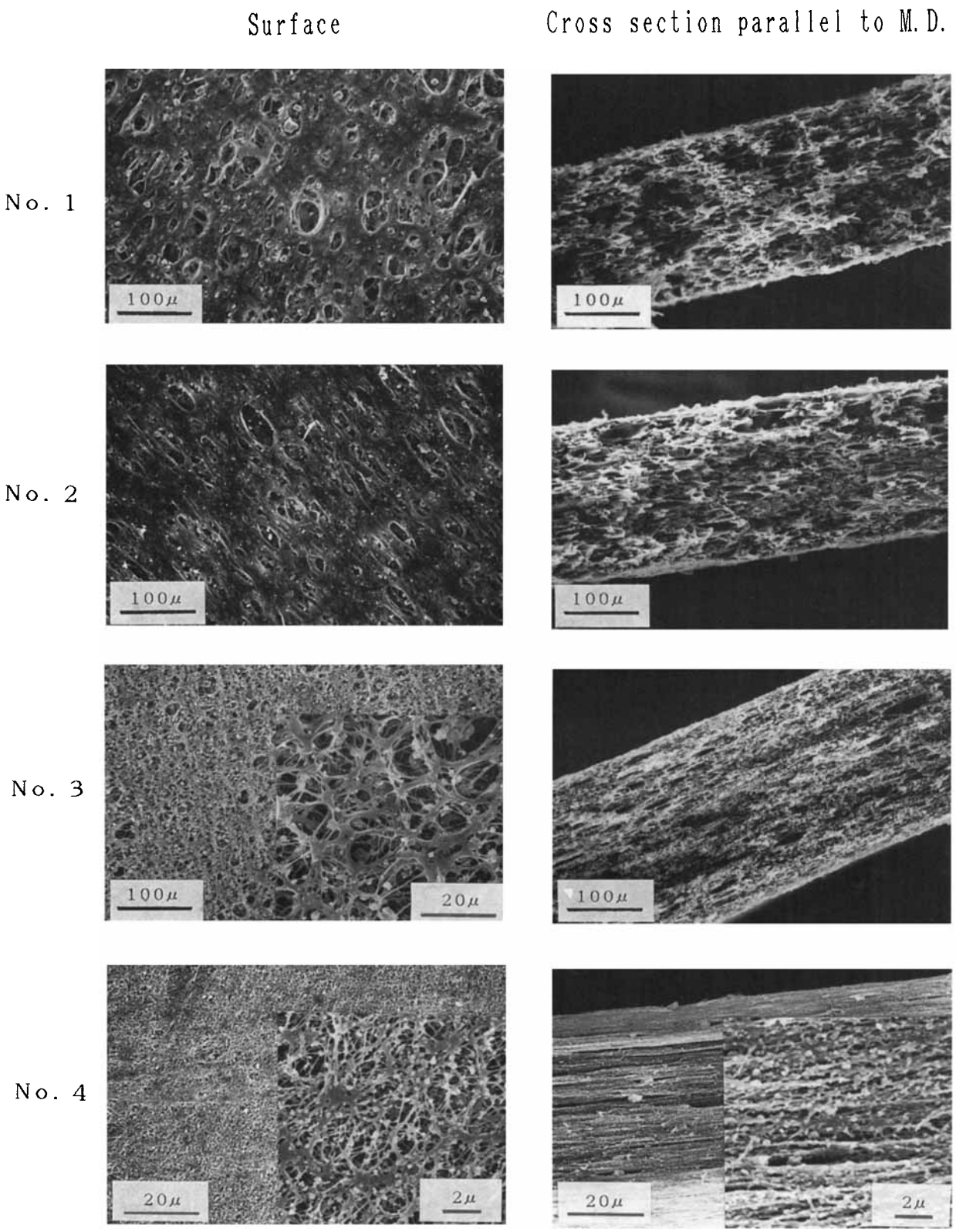

Figure 5 SEM photographs of biaxially stretched polypropylene microporous sheet. The mean particle size of $CaCO_3$ filler: No. 1, 3 μm; No. 2, 1.7 μm; No. 3, 0.8 μm; and No. 4, 0.08 μm.

Here, viscosity of N_2 gas at 20°C is 2.54×10^{-9} (psi/s). The term B_0 is the geometric factor of the membrane (cm^2); K_0 and B_0 can be calculated from a plot of K against $\bar{P}$.

The porosity (ϵ) and the tortuosity factor of pore (q) can be related to K_0 and B_0 by the following equation[7]:

$$K_0 = \left(\frac{4}{3}\right)\left(\frac{\delta}{k_1}\right)\left(\frac{\bar{v}}{q^2}\right)\epsilon m \tag{7}$$

$$B_0 = \left(\frac{m^2}{k}\right)\left(\frac{\epsilon}{q^2}\right) \tag{8}$$

δ/k_1 and k have been postulated as constant (0.8 and 2.5, respectively) as estimated by Carman.[8] The average molecular velosity ($\bar{v}$) of a gas (molecular weight, M) is given by

$$v = \left(\frac{8RT}{\pi M}\right)^{1/2} \tag{9}$$

The equivalent pore size m can be calculated by combining Eqs. (7), (8), and (9):

$$m = \left(\frac{16}{3}\right)\left(\frac{B_0}{K_0}\right)\left(\frac{2RT}{\pi M}\right)^{1/2} \tag{10}$$

Thus, Eq. (11) can be derived for measurement with N_2 gas at 20°C (293 K).

$$m = \frac{(1.256 \times 10^5 \text{ cm/s})B_0}{K_0} \tag{11}$$

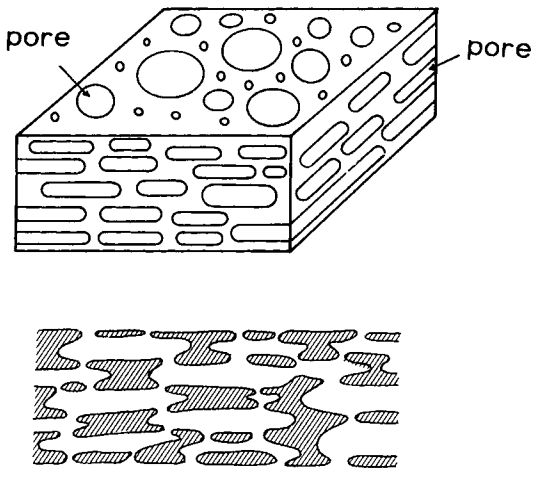

Figure 6 Schematic structure of microporous sheet.

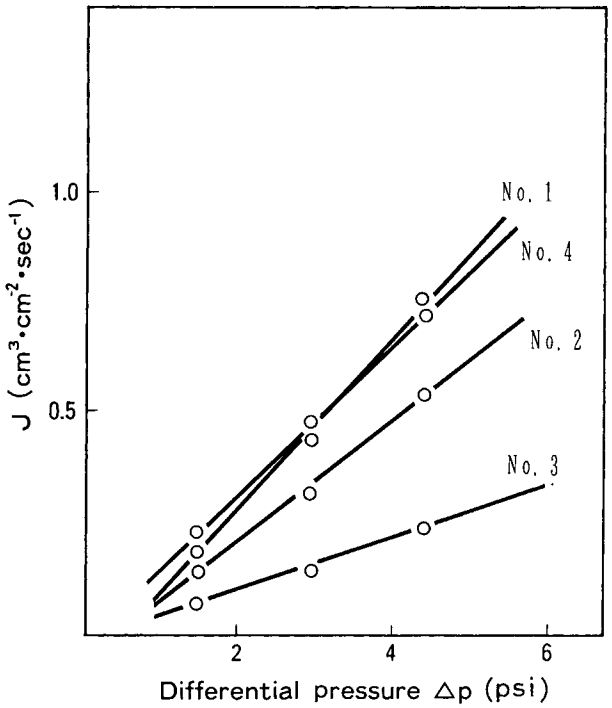

Figure 7 Dependency of N_2 gas flux (J) through the microporous sheet on pressure difference (ΔP).

Furthermore, the following equations are derived from Eqs. (7) and (9):

$$\frac{\epsilon}{q^2} = \frac{2.5B_0}{m^2} \tag{12}$$

$$q = 0.63m\left(\frac{\epsilon}{B_0}\right)^{1/2} \tag{13}$$

Thus, the effective porosity (ϵ/q^2) and the tortuosity factor of the pore (q) can be estimated.

RESULTS AND DISCUSSION

Microporous PP sheet is prepared by biaxially stretching the base sheet consisting of continuous PP phase and $CaCO_3$ filler particles, which are uniformly dispersed and filled in the PP phase.[15] The biaxial stretching engenders splitting of the continuous PP phase at the interface with the $CaCO_3$ particles and results in the microporous PP sheet. Table I shows the properties of the microporous PP sheet, prepared by using $CaCO_3$ fillers with various particle sizes. The decrease of the particle size makes the porosity of the sheet slightly larger and the maximum pore size smaller. Figure 4 shows the pore size

distribution curves of the microporous PP sheets. The smaller the mean particle size of the $CaCO_3$ filler, the smaller the pore size at the peak of the curve. All the distribution curves are pretty broad, especially in the range of the relatively larger pore size in the case of Nos. 1–3. The distribution curve in the case of No. 4 is almost symmetrical. These results described above are explainable as follows. The filler content was adjusted to be 59% by weight in this study. It means that the smaller the particle size of the filler, the larger the particle number of the filler. Therefore, the biaxial stretching results in the pore structure corresponding to the size and number of the filler particles filled in the base sheet. Namely, when the filler with relatively smaller particle size is used, the pore structure of the resultant microporous sheet is relatively finer.

Figure 5 shows scanning electron micrographs (SEM) of the surfaces and cross sections of the microporous sheets. The surfaces clearly show that the smaller the particle size of the filler, the smaller the pore size. On the other hand, the cross sections show a layered structure, which becomes finer with decreasing particle size of the filler. The reason the layered structure is formed is explicable as follows: the base sheet is stretched in the machine and transverse directions, two dimensionally, so void formation occurs after peeling at the interface between PP and $CaCO_3$ filler in the stretching directions. Accordingly, the stretched PP phase tends to form fine layers parallel to the stretching plane direction and, furthermore, the fine layers are three dimensionally interconnected with the fine PP strand. The smaller the particle size of $CaCO_3$ filler, the smaller the distance between the layers. Furthermore, these SEMs support the results and the mechanism of porous structure formation described above. Figure 6 shows the schematic structure of the microporous sheet.

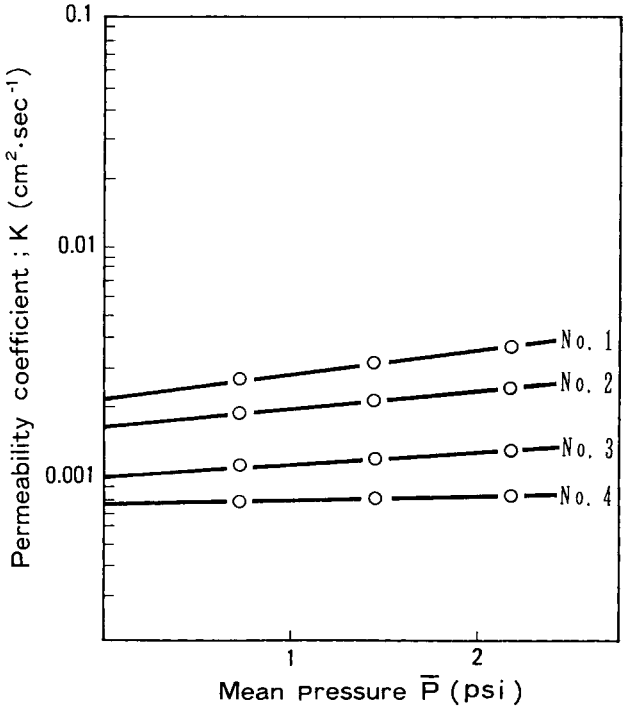

Figure 8 Relationship between mean pressure ($\bar{P}$) and permeation coefficient (K).

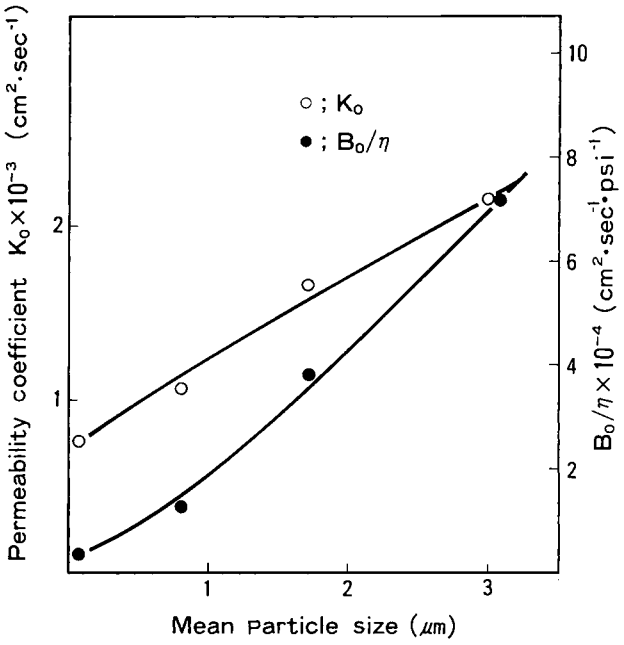

Figure 9 Relationship of permeability coefficient (K_0) and (B_0/η) to the mean particle size of fillers.

Figure 7 shows the dependency of N_2 gas flux (J) through the microporous PP sheet on pressure difference (ΔP). The higher the pressure difference, the larger the N_2 gas flux. There is a linear relation between the pressure difference. Permeability coefficients (K) of each samples can be calculated from the slopes of the lines shown in Figure 7.

Figure 8 shows the relationship between mean pressure ($\bar{P}$) and permeability coefficient (K). The higher the mean pressure ($\bar{P}$), the higher the permeability coefficient (K). The smaller the particle size of filler, the smaller the permeability coefficient (K). Knudsen permeability coefficient (K_0) and B_0/η can be calculated from the intercepts on vertical axis and slopes of the lines shown in Figure 8, re-

spectively. Figure 9 shows the calculated values of K_0 and B_0/η in relation to the particle size of $CaCO_3$ filler.

As the filler particle becomes relatively larger, K_0 and B_0/η increase, indicating the tendency that the pore of the sheet becomes relatively larger. The equivalent pore size (m) of the penetrating pore, through which N_2 gas is permeable, is obtained from Eq. (11) and B_0/η shown in Figure 9.

Figure 10 shows the comparison of the relations between mean particle size of $CaCO_3$ filler and pore size determined by various methods. All curves (A), (B), and (C) show a clear tendency that use of the filler with relatively smaller particle size of filler results in relatively smaller pore.

Figure 11 shows the dependence of effective porosity (ϵ/q^2) and tortuosity factor (q) on mean particle size of $CaCO_3$ filler, determined by Eqs. (12) and (13). As the particle size of filler becomes smaller, the effective porosity increases and, on the other hand, the tortuosity factor (q) decreases. This is probably explainable as follows. As the particle size of filler becomes smaller, the number of filler particles increases. Therefore, the number of pores formed by stretching increases, and the number of interconnecting pores also increases, consequently, the tortuosity factor decreases, with decreasing particle size of filler. The tortuosity factor (q) is 1 in the case that pore is cylindrical and perpendicular to the sheet surface.[10] Therefore, it is elucidated that the pore of the microporous PP sheets are pretty tortuous.

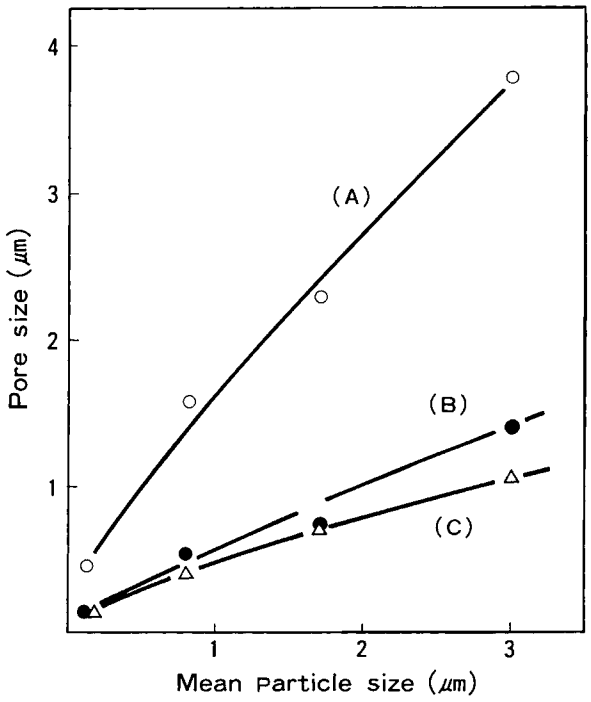

Figure 10 Comparison of the relations between mean particle size of $CaCO_3$ filler and pore size determined by various method: (A) maximum pore size; (B) pore size at peak position in pore distribution curve in Figure 4, and (C) equivalent pore size determined by permeability measurement.

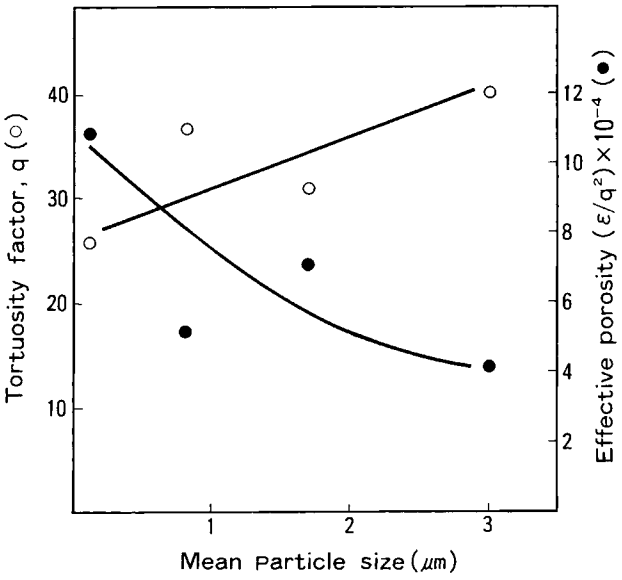

Figure 11 Dependence of effective porosity (ϵ/q^2) and tortuosity factor (q) on mean particle size of fillers.

CONCLUSION

For the biaxially stretched microporous sheet of polypropylene filled with $CaCO_3$ of four different mean particle diameters in the range 0.08–3.0 μm, keeping the amount of $CaCO_3$ (59 wt %) and the biaxial stretching ratio (2.8 × 1.8) constant, a relationship between the particle size of $CaCO_3$ and the structure of microporous sheet was examined by using a N_2 gas permeation method.

1. As the mean particle size of the filler becomes smaller, the effective porosity (ϵ/q^2) is increased.
2. The tortuosity factor (q) is in the range of 25–40 and shows the smaller the mean particle size of the filler, the smaller the tortuosity factor.
3. The equivalent pore size (m) becomes smaller with decreasing mean particle size.

REFERENCES

1. M. Shirai and Y. Kudō, *Jpn. Kokai Tokkyo Koho,* Sho 48-21749 (1973).
2. Y. Doi, S. Kaneko, and O. Fujii, *Jpn. Kokai Tokkyo Koho,* Sho 52-156776 (1977).
3. S. Tanaka, K. Yamauchi, and S. Kawai, *Jpn. Kokai Tokkyo Koho,* Sho 53-126319 (1978).
4. K. Kamata and T. Hirai, *Jpn. Kokai Tokkyo Koho,* Sho 53-38715 (1978).
5. R. G. Quynn and H. Brody, *J. Macromol. Sci.-Phys.,* **B5**(4), 721 (1971).
6. H. S. Birenbaum, R. B. Issacson, M. L. Druin, and S. G. Ploran, *Ind. Eng. Chem. Prod. Res. Develop.,* **13,** 2 (1974).
7. H. Yasuda and J. T. Tsai, *J. Appl. Polym. Sci.,* **18,** 805 (1974).
8. P. G. Carman, *Flow of Gas through Porous Media,* Butterworth, London, 1956.
9. I. Cabasso, K. Q. Robert, E. Klein, and J. K. Smith, *J. Appl. Polym. Sci.,* **21,** 1883 (1977).
10. Y. Shimizu, A. Tanioka, K. Miyasaka, and K. Ishikawa, *J. Polym. Sci. Phys.,* **17,** 1495 (1979).
11. Y. Mizutani, K. Kusumoto, S. Nakamura, and Y. Mizumoto, *Jpn. Kokai Tokkyo Koho,* Sho 53-21426 (1978).
12. S. Nakamura, K. Okamura, S. Kaneko, T. Fujii, and T. Sumiura, *Jpn. Kokai Tokkyo Koho,* Sho 58-38304 (1983).
13. S. Nakamura, K. Okamura, S. Kaneko, and Y. Mizutani, *Kobunshi Ronbunshu,* **48,** 463 (1991).
14. S. Nakamura, K. Okamura, and Y. Mizutani, *Kobunshi Ronbunshu,* **48,** 491 (1991).
15. S. Nagō, S. Nakamura, and Y. Mizutani, *J. Electron Microscopy,* to appear.

Received May 28, 1991
Accepted September 23, 1991